NASA Technical Memorandum 87311

The Cyclic Stress-Strain Behavior of PWA 1480 at 650 °C

T.P. Gabb
Lewis Research Center
Cleveland, Ohio

and

G.E. Welsch
Case Western Reserve University
Cleveland, Ohio

Prepared for the
1986 TMS-AIME Annual Meeting
New Orleans, Louisiana, March 2–6, 1986

NASA

THE CYCLIC STRESS-STRAIN BEHAVIOR OF PWA 1480 AT 650 °C

T.P. Gabb
National Aeronautics and Space Administration
Lewis Research Center
Cleveland, Ohio 44135

and

G.E. Welsch
Case Western Reserve University
Dept. of Metallurgy and Materials Science
Cleveland, Ohio 44106

E-3038

SUMMARY

The monotonic plastic flow behavior of several single crystal nickel-base superalloys has been shown to vary significantly with crystallographic orientation. In the present study, the cyclic plastic flow response of one such alloy, PWA 1480, was examined at 650 °C in air. Single crystal specimens aligned near several crystallographic directions were tested in fully reversed, total-strain-controlled low cycle fatigue tests at a frequency of 0.1 Hz. The cyclic stress-strain response and general cyclic hardening behavior was analyzed as a function of crystallographic orientation and inelastic strain range.

INTRODUCTION

Examinations of the monotonic tensile and fatigue behaviors of the single crystal nickel-base superalloys René N4 (refs. 1 and 2) and PWA 1480 (refs. 3 and 4) have disclosed orientation-dependent tension-compression anisotropies (TCA) and significant differences in the mechanical response of octahedral and cube slip at intermediate temperatures. The monotonic tensile yielding behavior parallels that of single phase $Ni_3(Al,Nb)$ in some aspects which can be explained using the model of Lall, Chin, and Pope (ref. 5). There have been some indications that these alloys may also have similarities in cyclic hardening response. In examining such behavior it is informative to isolate orientation effects while slip occurs only on a single slip system. The purpose of this study is to examine the cyclic hardening response of the single crystal superalloy PWA 1480 at 650 °C where the tension-compression anisotropy is present, primarily under conditions where only a single slip system is operative.

EXPERIMENTAL CONDITIONS

The PWA 1480 single crystals tested had the nominal composition in weight percent of 10Cr, 5Co, 4W, 12Ta, 5Al, 1.5Ti, and balance Ni. The heat treated alloy contained about 65 vol % of cuboidal γ' particles of about 0.6±0.1 μm on edge dimension, (fig. 1). This particle size was significantly larger than that quoted elsewhere of 0.4 μm, (refs. 3 and 4). This is probably due to a somewhat lower solution temperature, (1275 versus 1288 °C) and slower cooling rate for the material employed in the present study. Specimens with stress axes near [001], [011], [$\bar{1}$11], [$\bar{2}$ 5 20], [$\bar{3}$ 6 10], and [$\bar{2}$ 3 4] crystallographic

orientations (fig. 2) were machined from cast single crystal slabs. Actual crystallographic orientations were determined within ±2° for each specimen. Low cycle fatigue (LCF) and tensile tests were performed at 650 °C for each specimen orientation in a servohydraulic testing machine. Heating was supplied by a clamshell furnace. The majority of the LCF tests were performed with constant total axial strain amplitude using a 0.1 Hz sinusoidal strain control waveform. Additional LCF tests were performed at a constant inelastic strain range by continuously adjusting the total strain range as required. The LCF tests were randomly started in either tension or compression in the first half cycle. Tensile tests were performed at a constant strain rate or at a constant displacement rate chosen to give strain rates comparable to that of the LCF tests. Load and strain were continuously recorded on a strip chart recorder. The load signal was also independently monitored with a digital multimeter. Hysteresis loops were periodically recorded on an X-Y recorder. In order to establish the absence of extensometer slippage, several tests were duplicated: (a) on the same test machine with specimens having deep surface scratches to prevent probe slip; (b) on an entirely different test machine employing diameteral extensometry and direct resistance heating on hourglass-shaped specimens of [001] orientation.

The operative slip systems were determined after testing by measuring the orientation of slip traces in tensile and LCF specimens and by determining the rotation of the tensile axis towards the slip direction in tensile tests. In addition, TEM foils were prepared from the LCF specimens and examined in a Phillips EM400T at 120 kV in order to determine dislocation burgers vectors and slip planes.

RESULTS

The yield strengths in tension and compression are listed in table I. Primarily due to the larger γ' size (ref. 3), these values are about 10 percent lower than that observed elsewhere (refs. 3 and 4). The tension-compression anisotropy was comparable to that in these other studies. Specimens with orientations near [011], [$\bar{2}$ 5 20], and [$\bar{3}$ 6 10] displayed single slip on the primary octahedral [$\bar{1}$01](111) slip system and moderate initial jerky flow, while the [$\bar{2}$ 3 4] specimens had single slip on the primary cube [$\bar{1}$10](001) system and minor jerky flow. The jerky flow abated at the onset of strain hardening in both the tensile and LCF tests, suggesting a similar strain hardening mechanism. Specimens oriented along [001] and [$\bar{1}$11] showed evidence of slip on multiple octahedral and cube slip systems respectfully, and little or no jerky flow.

Deformation by Single Slip

The number of slip traces observed in the LCF tests of single slip specimens was roughly proportional to the initial inelastic strain range. Distinct slip steps were present on the surface of specimens displaying octahedral slip, while specimens displaying primary cube slip had less distinct slip traces on a relatively smooth surface. Preliminary analysis of the TEM foils disclosed that essentially all dislocations in primary octahedral slip specimens were of the corresponding burgers vector, 1/2[$\bar{1}$01], and slip plane (111). Specimens displaying primary cube slip only had about 70 percent of the dislocations with the corresponding burgers vector, 1/2[$\bar{1}$10], and slip plane (001).

The LCF test results are listed in table II and the cyclic stress and inelastic strain response in a typical LCF test of a specimen deforming by single slip is shown in figure 3. A polynomial description of inelastic strain range data as a function of fatigue cycles, of the form $\Delta\varepsilon_{in} = A + BN + CN^2 + DN^3 + EN^4 + F \ln N$, was generated for use in calculating the cumulative shear strain in LCF tests. This enabled comparison of the resolved shear stress versus cumulative shear strain response in the various LCF tests with that of tensile tests. The resulting $\tau_t - \gamma_c$ curves of typical LCF and tensile tests are depicted for the [$\bar{2}$ 5 20], [$\bar{3}$ 6 10], [0 1 1], and [$\bar{2}$ 3 4] specimens in figures 4 to 7. The tensile and LCF strain hardening curves of the [$\bar{2}$ 5 20], [$\bar{3}$ 6 10], and [0 1 1] octahedral slip specimens all displayed a comparable Stage I easy glide region of very little strain hardening which extended out to a cumulative strain value of about 7.5 percent. This maximum easy glide strain value marked the cessation of jerky flow and the onset of more rapid, stable strain hardening. The [$\bar{2}$ 3 4] cube slip specimens did not show this correspondence (fig. 7) as these LCF specimens did not display this response.

The dependency of cyclic resolved shear stress on inelastic strain amplitude at half of cyclic life is depicted in figure 8. The response was quite comparable for all specimens displaying single slip. The stress amplitude was very nearly independent of inelastic strain amplitude in these tests, with a cyclic strain hardening coefficient of essentially zero (0.03±0.02).

Cyclic Hardening Anisotropy in Tension and Compression

In LCF tests of large inelastic strain range significant anisotropy of the cyclic hardening in tension versus compression was sometimes observed which seemed to vary systematically with crystallographic orientation. Others (ref. 10) have found this effect was accentuated in constant inelastic strain range tests. Several specimens were tested in this fashion. The cyclic stress response in one of these tests is shown in figure 9. The difference in hardening response in tension and compression is clearly evident. This cyclic hardening anisotropy can also be illustrated by plotting the mean stress $\tau_m = (\tau_{max} - \tau_{min})/2$, normalized by the stress range $\Delta\tau = \tau_{max} + \tau_{min}$, versus the number of fatigue cycles. This is shown in figure 10 for both single slip and multiple slip specimens. The hardening anisotropy was consistently in the high strength direction for specimens displaying octahedral slip. The [001] specimens had a higher yield strength in tension and cyclically hardened more in tension, while the [$\bar{3}$ 6 10] and [0 1 1] specimens had a higher yield strength in compression and cyclically hardened more in that direction. Both cube slip specimens cyclically hardened more in compression, irregardless of initial tension-compression anisotropy. The shear stress amplitude-cumulative shear strain curves of single slip specimens tested in this manner, shown in figure 11, were comparable to those found in the earlier tests, (figs. 4 to 7).

DISCUSSION

Slip on a single slip system was clearly the preferred plastic deformation mode at 650 °C for specimens with stress axis oriented more than 10° away from the [001] and [$\bar{1}$11] crystal orientations. There were significant differences between octahedral and cube slip. Specimens deforming in octahedral slip on a

single system had similar initial hardening responses in tensile and LCF tests. The hardening curves of these specimens each contained an easy glide region extending to a cumulative shear strain of about 7.5 percent. This regime was characterized by jerky flow in the tensile and LCF tests. The fact that the maximum easy glide strain value in these tests was relatively independent of unidirectional or reversed loading path, inelastic LCF strain range, and specific crystallographic orientation seems to indicate this deformation is somewhat irreversible, as a characteristic, direction-independent amount of deformation seems necessary to initiate Stage II strain hardening. The subsequent Stage II hardening was significantaly higher in tensile tests than in tensile tests, and may not be directly related.

Specimens displaying cube slip on a single system did not have similar tensile and LCF hardening curves. While tensile tests displayed an easy glide regime, all LCF tests displayed Stage II strain hardening from the first cycle. So primary cube slip seems to involve a different deformation mechanism compared to octahedral slip, with dependencies on unidirectional versus reversed loading.

The cyclic stress-strain curves of all single slip specimens at half of cyclic life disclosed very little stress dependency on inelastic strain amplitude over the range of tests performed. This has also been observed in single crystal copper (ref. 7) and in single crystal MAR-M200 at room temperature (ref. 8). It has been associated with heterogeneous deformation in persistent slip bands, with the constant stress corresponding to the shear stress required to form these bands. Such an interpretation may be applicable here, although TEM examination disclosed a slip direction texture in the dislocation structure rather than discrete slip bands. But the converse is not always true, as René N4 single crystals cycled at 760 °C do display significant cyclic strain hardening with slip bands superimposed on a general deformation structure quite comparable to that observed here (ref. 10).

The TCA in cyclic hardening of specimens displaying octahedral slip clearly varied directly with initial monotonic tension-compression yield strength anisotropy. This was previously observed in René N4 (ref. 2) at 760 °C and has also been observed in single phase γ' (refs. 9 and 6). In those studies, the [011] specimens displayed the greatest cyclic hardening anisotropy, as also seen here. So, at intermediate temperatures the analogies in the stress-strain response of single crystal γ' and Ni-base superalloys such as PWA 1480 and Rene N4 seem to extend to cyclic deformation also, as the mechanical response is controlled by γ' precipitate shearing. As in these other studies, the cyclic anisotropy was only significant in total strain controlled and inelastic strain controlled tests of large inelastic strain amplitudes, where screw dislocation storage is prevalent in the γ' precipitates (ref. 10). The application of the TCA model of Lall, Chin, and Pope (ref. 5) predicts a higher yield strength and greater cyclic hardening in the loading direction which encourages irreversible cross slip of the lead dislocation of a dislocation pair from the (111) to the (010) plane (11).

It is also significant that both PWA 1480 and René N4 specimens which deform by cube slip display a substantially different TCA from that in octahedral slip. This cube slip TCA seems to invariably encourage greater compressive cyclic hardening at intermediate temperatures, and shows an independent, more complex temperature dependence than that in octahedral slip (ref. 2).

CONCLUSIONS

1. PWA 1480 single crystal specimens oriented away from the [001] and [$\bar{1}$11] crystallographic orientations deform by single slip in tensile and LCF tests at 650 °C.

2. Specimens deforming by octahedral slip on a single slip system have similar hardening response in tensile and LCF loading.

3. Octahedral slip specimens tested in high inelastic strain LCF tests displayed significant cyclic tension-compression anisotropic hardening which varied proportionally with initial monotonic TCA, as has been observed for single phase γ'.

4. Specimens deforming by cube slip have dissimilar tensile and LCF hardening curves, and tend to cyclically harden more in compression, suggesting a different hardening mechanism from that in octahedral slip.

5. Cyclic strain hardening is very low for specimens displaying single slip.

ACKNOWLEDGEMENTS

The authors wish to acknowledge the many helpful discussions with R.V. Miner, J. Gayda, and R.A. MacKay, NASA Lewis Research Center.

REFERENCES

1. R.V. Miner, T.P. Gabb, J. Gayda, and K.J. Hemker: Metall. Trans. A, 1986, vol. 17A, pp. 507-512.

2. T.P. Gabb, J. Gayda, and R.V. Miner: Metall. Trans. A, 1986, vol. 17A, pp. 497-505.

3. D.M. Shah, and D.N. Duhl: in Superalloys 1984, M. Gell, C.S. Kortovich, R.H. Bricknell, W.B. Kent and J.F. Radavich, eds., pp. 105-114, The Metallurgical Society of AIME, Warrendale, PA, 1984.

4. F.E. Heredia, and D.P. Pope: Acta Metall., 1986, vol. 34, pp. 279-285.

5. C. Lall, S. Chin, and D.P. Pope: Metall. Trans., A, 1979, vol. 10A, pp. 1323-1332.

6. S.S. Ezz, and D.P. Pope: Scr. Metall., 1985, vol. 19, pp. 741-745.

7. A.S. Cheng, and C. Laird: Mater. Sci. Eng., 1981, vol. 51, pp. 111-121.

8. L.G. Fritzemeier: "The Cyclic Stress-Strain Behavior of Nickel-Base Superalloy Poly- and Single Crystals," Ph.D. Thesis, Columbia University, 1984.

9. H.R. Pak, L.M. Hsiung, and M. Kato: in High-Temperature Ordered Intermetallic Alloys, C.C. Koch, C.T. Liu, and N.S. Stoloff, eds., pp. 239-246, Materials Research Society, Pittsburgh, 1985.

10. T.P. Gabb, R.V. Miner, and J. Gayda: Scr. Metall., 1986, vol. 20, pp. 513-518.

11. S.S. Ezz, and D.P. Pope: Scr. Metall., 1982, vol. 16, pp. 117-118.

TABLE I. - MONTONIC YIELD STRENGTH OF THE TEST MATERIAL

[h k l]	Tension 0.02 percent offset, MPa	Tension 0.2 percent offset, MPa	Compression 0.02 percent offset, MPa
0 0 1	868	965	776
0 1 1	801	818	897
$\bar{1}$ 1 1	732	752	710
$\bar{2}$ 5 20	828	855	818
$\bar{3}$ 6 10	733	745	785
$\bar{2}$ 3 4	727	740	744

TABLE II. - LCF TEST RESULTS

Orientation h k l	Cyclic stress-strain response, cycle 1/.5 N_f				Maximum easy glide strain γ_g, percent	Fatigue life N_f, cycles
	Total strain range $\Delta\gamma$, percent	Inelastic strain range $\Delta\gamma$, percent	Maximum stress τ_{max}, MPa	Minimum stress τ_{min}, MPa		
[0 0 1]	[a]4.20/4.56	0.24/0.24	374/419	362/387	----	192
[$\bar{1}$ 18 20]	2.11/2.11	.14/.09	373/376	391/400	----	824
[$\bar{1}$ 9 10]	2.22/2.22	.32/.16	355/367	395/417	4.5	976
[$\bar{3}$ 19 20]	2.65/2.65	.67/.25	354/398	389/455	7.0	555
[$\bar{1}$ 19 20]	[a]2.38/2.64	.24/.24	352/372	386/434	10.0	577
[$\bar{1}\bar{5}$ 17 20]	[a]1.27/1.59	.20/.20	370/436	362/470	----	413
[$\bar{1}$ 5 20]	3.10/3.10	.19/.10	422/428	395/405	5.5	427
[$\bar{3}$ 5 20]	3.05/3.05	.31/.17	404/420	385/396	10.0	237
[$\bar{1}$ 1 10]	3.83/3.83	.61/.29	393/427	368/396	6.0	165
[$\bar{5}$ 11 20]	1.90/1.90	.27/.14	368/371	380/391	9.0	1171
[$\bar{3}$ 7 10]	2.07/2.07	.36/.19	348/370	364/388	7.0	971
[$\bar{6}$ 11 20]	2.18/2.18	.52/.25	373/412	381/428	6.0	180
[$\bar{7}$ 13 20]	[a]2.05/2.36	.22/.22	348/378	363/415	8.5	723
[$\bar{2}$ 3 4]	1.53/1.53	.17/.06	359/379	365/396	----	2063
[$\bar{9}$ 15 20]	1.67/1.67	.27/.10	355/398	375/402	----	1200
[$\bar{9}$ 18 20]	1.82/1.82	.46/.19	349/412	377/435	----	281
[$\bar{7}$ 17 20]	[a]1.60/1.97	.22/.22	340/392	353/437	----	215
					$\bar{\gamma}_g$ = 7.4±1.9	

[a]Constant inelastic strain range test.

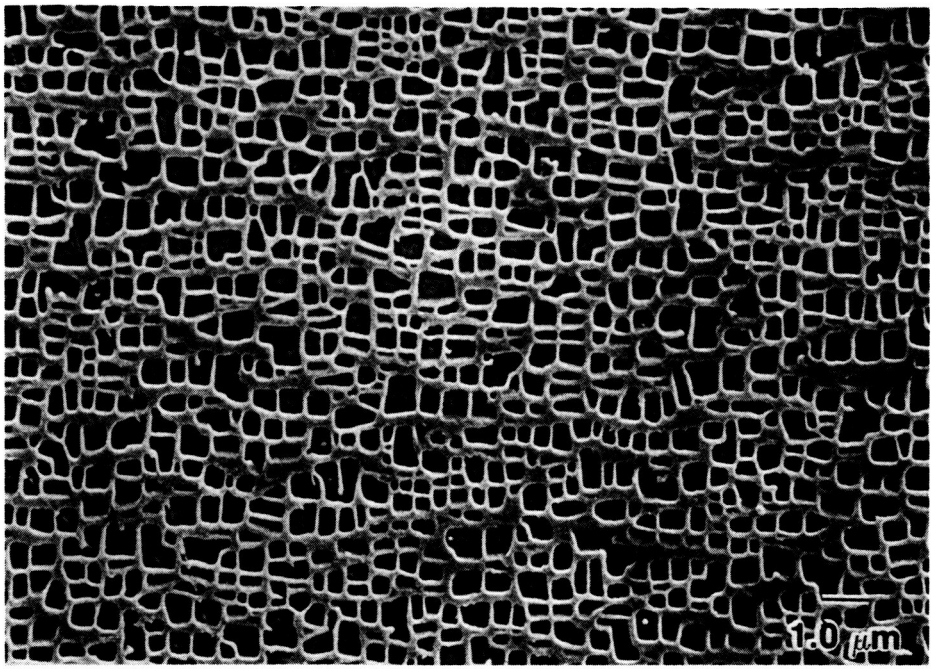

Figure 1. - Test material microstructure.

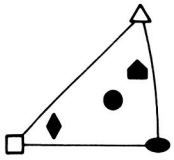

♦ $[\bar{2}\ 5\ 20]$ PRIMARY OCTAHEDRAL SLIP
● $[\bar{3}\ 6\ 10]$ PRIMARY OCTAHEDRAL SLIP
⬬ $[0\ 1\ \ 1]$ PRIMARY OCTAHEDRAL SLIP
▲ $[\bar{2}\ 3\ \ 4]$ PRIMARY CUBE SLIP

SINGLE SLIP VERIFICATION AND ANALYSIS

- TENSILE TESTS
  - TENSILE AXIS ROTATION
  - SLIP TRACES
- LCF TESTS
  - SLIP TRACES
- TEM
  - BURGERS VECTOR AND SLIP PLANE OF DISLOCATIONS

Figure 2. - Crystallographic orientations examined.

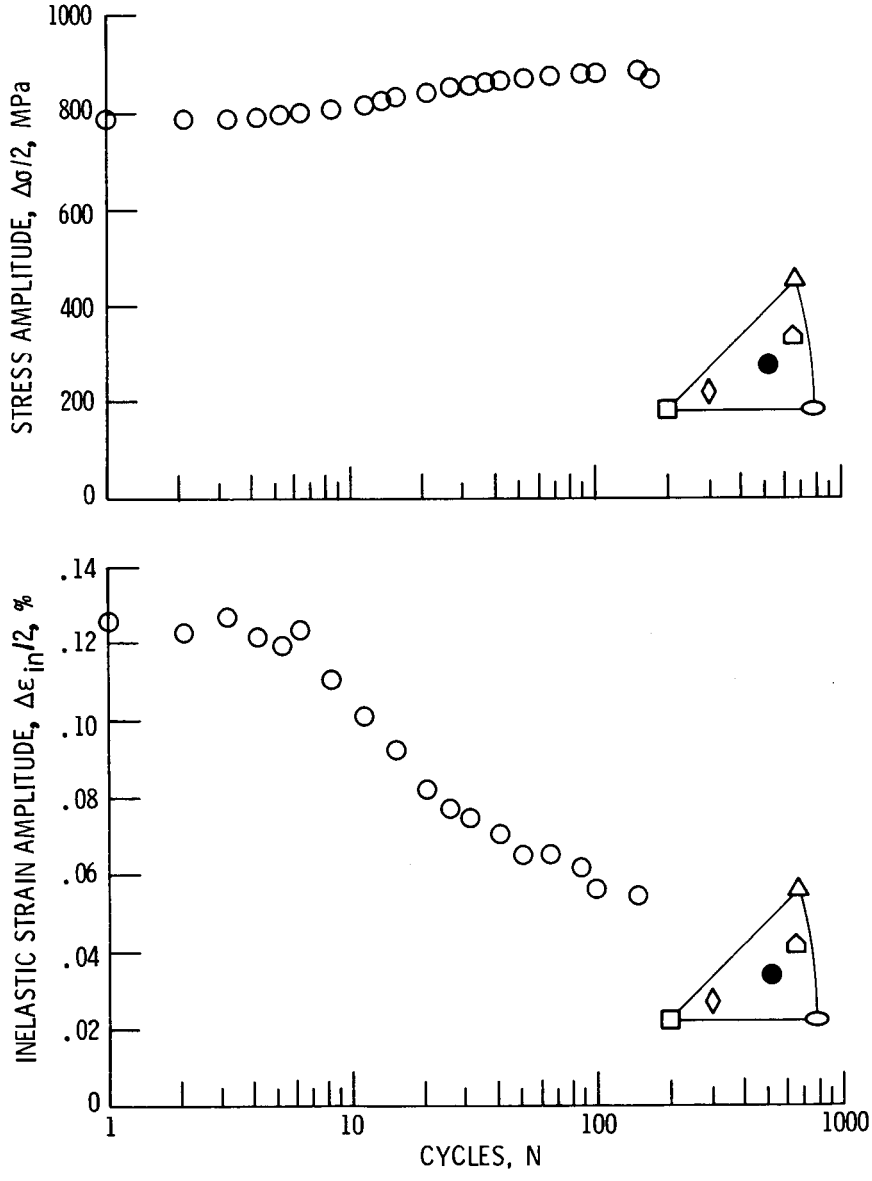

Figure 3. - Typical cyclic stress-strain response.

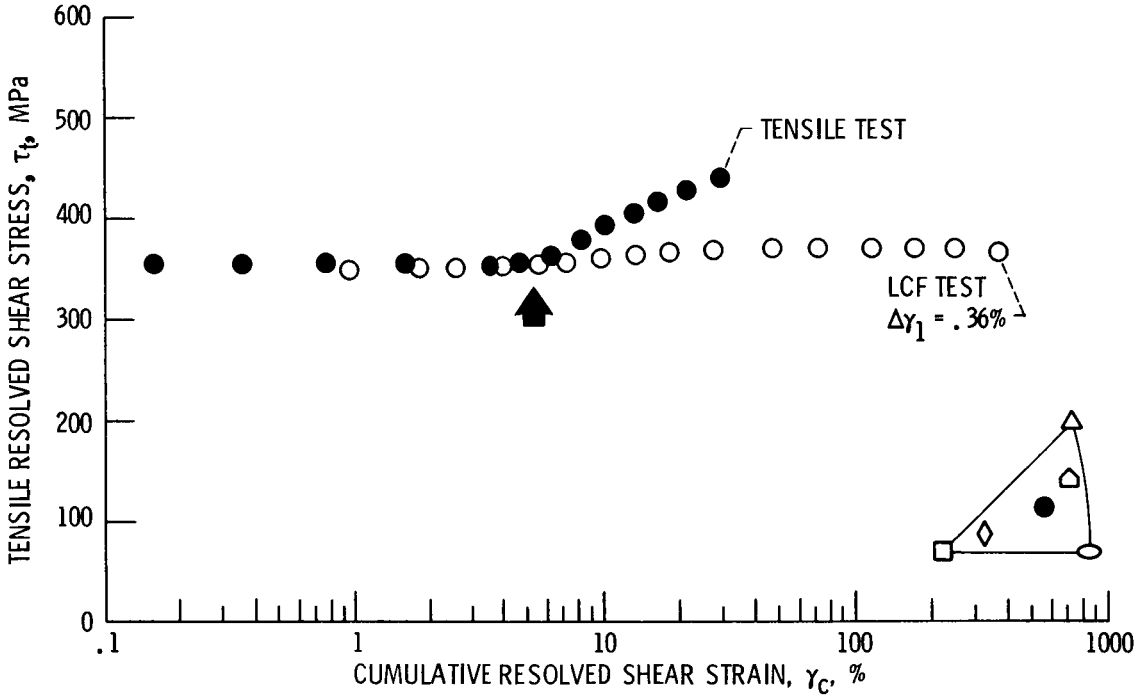

Figure 4. - Hardening response of [$\bar{3}$ 6 10] specimens.

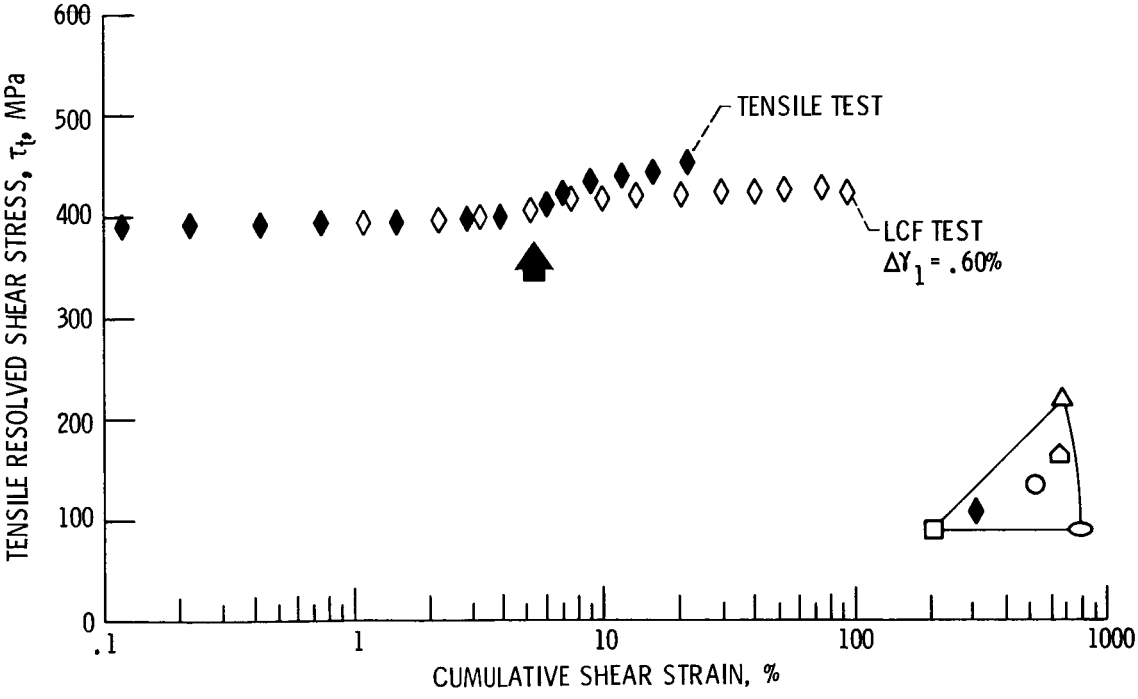

Figure 5. - Hardening response of [$\bar{2}$ 5 20] specimens.

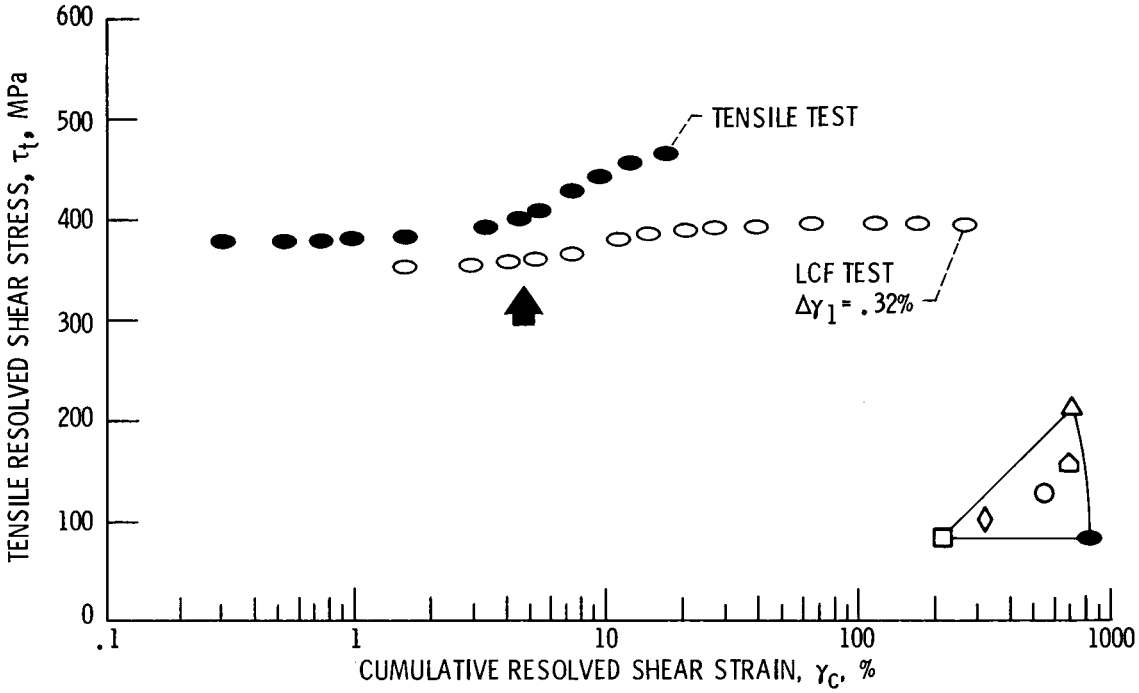

Figure 6. - Hardening response of [0 1 1] specimens.

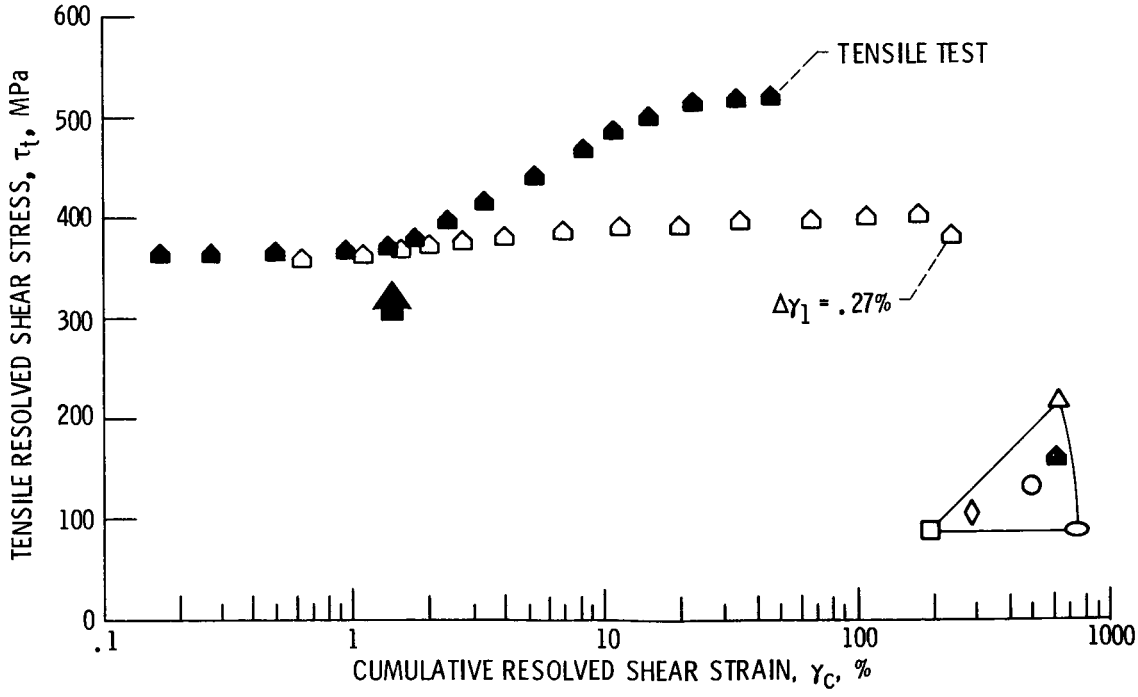

Figure 7. - Hardening response of [$\bar{2}$ 3 4] specimens.

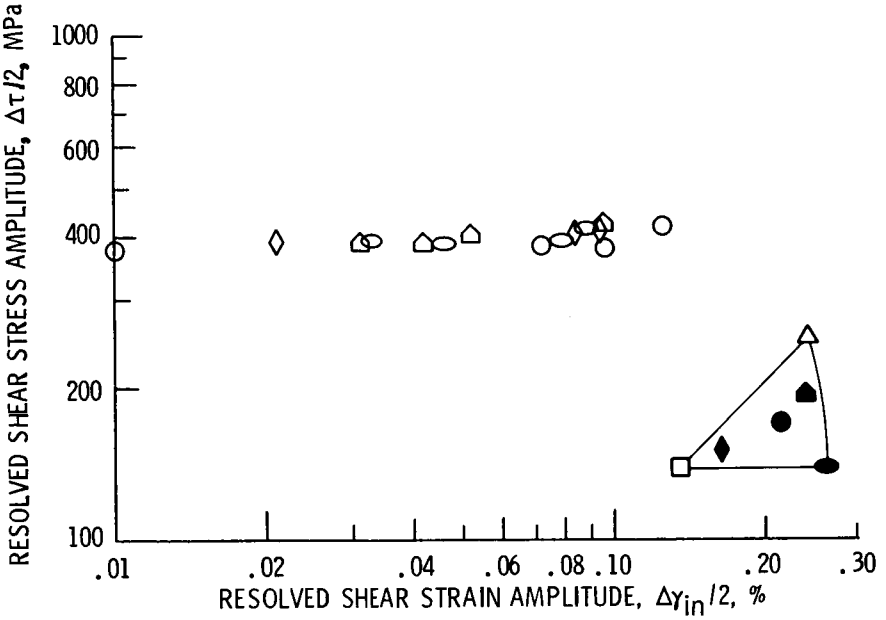

Figure 8. - Cyclic stress-strain curve at half-life.

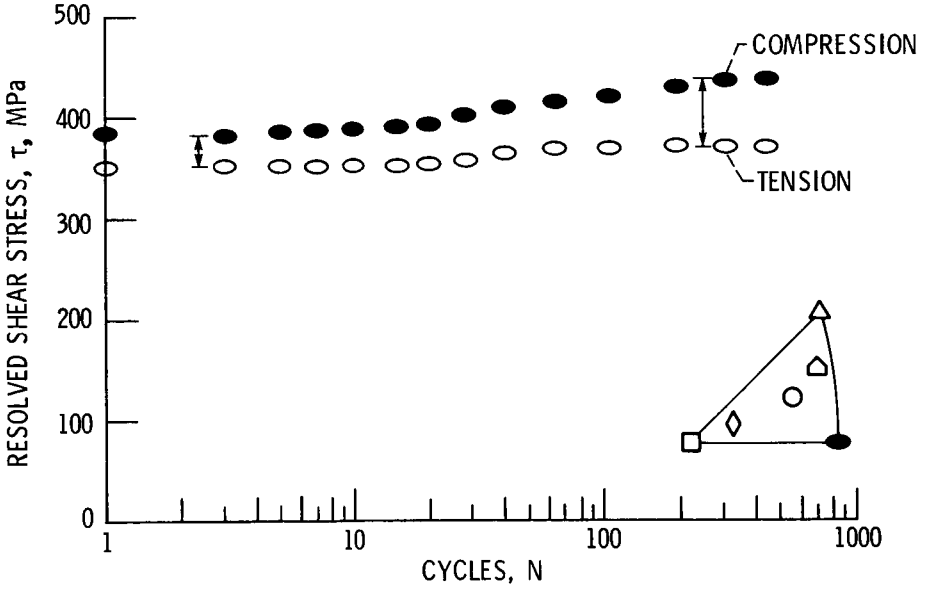

Figure 9. - Tensile vs. compressive cyclic hardening, [0 1 1] specimen.

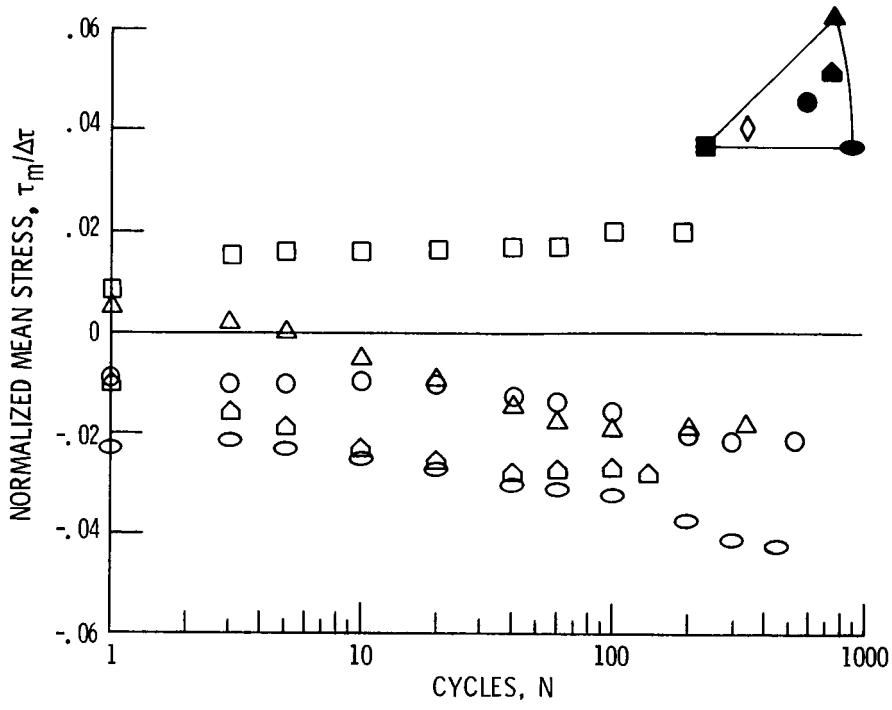

Figure 10. - Mean stress in constant inelastic strain range tests.

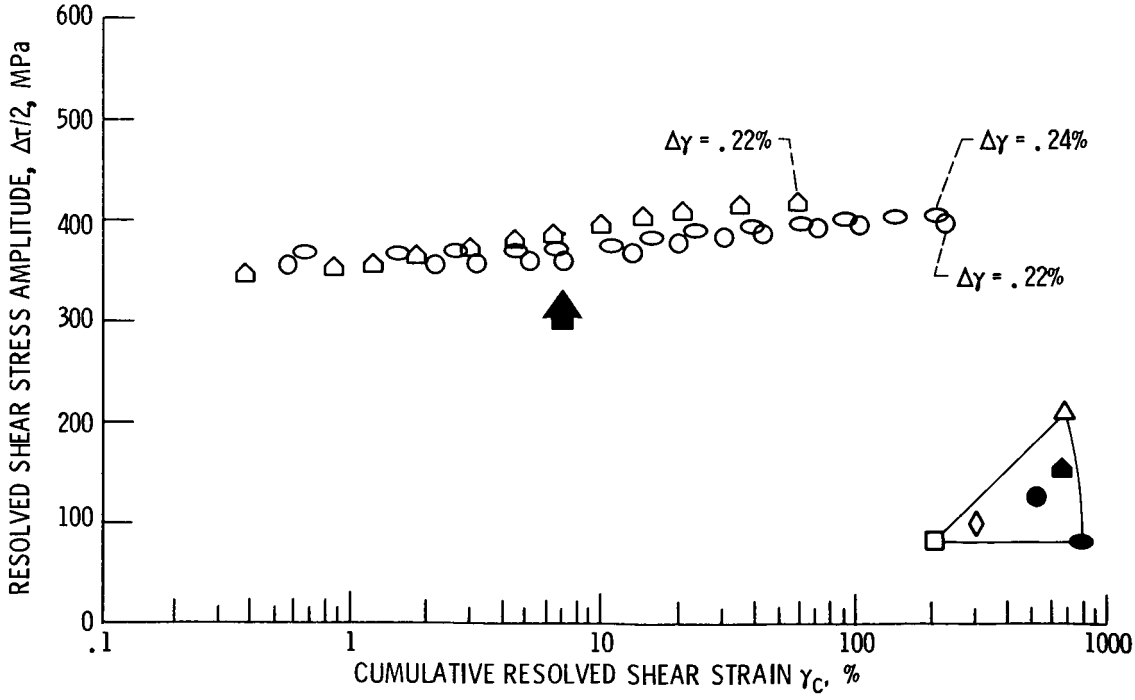

Figure 11. - Cyclic hardening in constant inelastic strain range tests.

1. Report No.	2. Government Accession No.	3. Recipient's Catalog No.
NASA TM-87311		

4. Title and Subtitle	5. Report Date
The Cyclic Stress-Strain Behavior of PWA 1480 at 650 °C	6. Performing Organization Code: 505-63-01

7. Author(s)	8. Performing Organization Report No.
T.P. Gabb and G.E. Welsch	E-3038
	10. Work Unit No.

9. Performing Organization Name and Address	11. Contract or Grant No.
National Aeronautics and Space Administration Lewis Research Center Cleveland, Ohio 44135	13. Type of Report and Period Covered: Technical Memorandum

12. Sponsoring Agency Name and Address	14. Sponsoring Agency Code
National Aeronautics and Space Administration Washington, D.C. 20546	

15. Supplementary Notes

Prepared for the 1986 TMS-AIME Annual Meeting, New Orleans, Louisiana, March 2-6, 1986. T.P. Gabb, NASA Lewis Research Center; G.E. Welsch, Case Western Reserve University, Dept. of Metallurgy and Materials Science, Cleveland, Ohio 44106.

16. Abstract

The monotonic plastic flow behavior of several single crystal nickel-base superalloys has been shown to vary significantly with crystallographic orientation. In the present study, the cyclic plastic flow response of one such alloy, PWA 1480, was examined at 650 °C in air. Single crystal specimens aligned near several crystallographic directions were tested in fully reversed, total-strain-controlled low cycle fatigue tests at a frequency of 0.1 Hz. The cyclic stress-strain response and general cyclic hardening behavior was analyzed as a function of crystallographic orientation and inelastic strain range.

17. Key Words (Suggested by Author(s))	18. Distribution Statement
Single crystal; Superalloy; Low cycle fatigue	Unclassified - unlimited STAR Category 26

19. Security Classif. (of this report)	20. Security Classif. (of this page)	21. No. of pages	22. Price*
Unclassified	Unclassified		

*For sale by the National Technical Information Service, Springfield, Virginia 22161